Efficient Computation of the Lifetime Reliability of Deteriorating Structures

Hyun-Joong Kim
Senior Researcher, Korea Bridge Design & Engineering Research Center, Seoul National University, Seoul, South Korea

Daniel Straub
Professor, Engineering Risk Analysis Group, Technische Universität München, Munich, Germany

ABSTRACT: This paper proposes two computation schemes for efficient evaluation of sets of reliability analyses associated with different time intervals. The first approach is based on sequential solving the reliability analyses starting from the last time interval. It enables to use the solution of a time interval as a starting point and to efficiently solve the reliability problem of preceding time intervals. Its implementation combined with Subset Simulation (SuS) and Sequential Importance Sampling (SIS) is presented. The second proposed approach is centered around reformulating the limit state function in a way that the time to failure can be described. This allows to efficiently obtain the estimates of failure probabilities and corresponding time intervals by one run of SuS. The numerical verification demonstrates that the proposed methods are capable of obtaining accurate estimates of lifetime reliability with a substantially reduced computational cost.

1. INTRODUCTION

Exact calculation of lifetime reliability of deteriorating structures in the general case requires the computation of a first-passage probability (Rackwitz 1998; Andrieu-Renaud et al. 2004; Lentz et al. 2004; Melchers and Beck 2018), which can be associated with significant computational cost. Under some circumstances, the problem can be approximated by transforming it into a series of time-invariant reliability problems associated with discretized time intervals, e.g. yearly or monthly periods (e.g., Val and Melchers 1997; Schneider et al. 2017; Kim and Straub 2019). While these are conceptually easier and computationally cheaper to solve, they may still lead to significant computation cost because one needs to evaluate reliability problems for all time intervals; this motivates the use of efficient computation schemes. In particular, the similarity among failure events in different time intervals can be exploited to enhance the computational efficiency.

This contribution presents two schemes for efficient evaluation of the series of reliability analyses associated with different time intervals. These are applicable to the lifetime reliability analysis of deteriorating structures whose resistance decreases monotonically and in which load effects can be modeled as a stationary process.

The first approach is based on solving the reliability analyses sequentially, starting from the last time interval. By projecting the series of time-invariant problems onto an equivalent outcome space, the solution at one time interval can be used as a starting point to solve the reliability problem at preceding time intervals. This strategy is particularly efficient when employing sequential sampling-based methods, and is here implemented with Subset Simulation (SuS) and Sequential Importance Sampling (SIS).

The second proposed approach is centered around solving the limit state function for t. This allows for an efficient use of SuS, in which the

parameter t takes the role of the threshold value defining the intermediate subsets.

The performance of both approaches is investigated through a numerical example.

2. SEQUENTIAL RELIABILITY ANALYSIS BASED ON BACKWARD CALCULATION

2.1. Interval and cumulative failure events

We discretize time in intervals $j = 1,2,\dots,M$ such that the j th interval corresponds to $t \in (t_{j-1}, t_j]$. Failure in interval j is only possible if the structure has not failed previously. For this reason, the computation of the probability of failure in interval j must account for the entire history leading up to t_{j-1}. This is represented by the *cumulative failure event*, $F(t_j)$, which is:

$$F(t_j) = \left\{ \min_{\tau \in [0,t_j]} g(\mathbf{X}, \tau) \leq 0 \right\} \tag{1}$$

wherein $\mathbf{X}$ is the random vector that comprises uncertain variables affecting the failure. We call its probability $\Pr[F(t_j)]$ the cumulative failure probability.

To facilitate computation, we work with the *interval failure event*, F_j^*, which neglects the history, i.e. it describes a failure of the structure in the interval j ignoring possible earlier failures (for details see Straub et al. 2019). It is

$$F_j^* = \left\{ \min_{\tau \in (t_{j-1},t_j]} g(\mathbf{X}, \tau) \leq 0 \right\} \tag{2}$$

The corresponding $\Pr(F_j^*)$ is the interval failure probability. When the loads S and the capacity R are separable in $\mathbf{X}$, it is possible to approximate it as

$$\Pr(F_j^*) \approx \Pr[R(t_j) \leq S_{max,j}] \tag{3}$$

wherein $S_{max,j}$ is the maximum load effect in time interval j. Note that, in the general case, F_j^* is not a subset of F_{j+1}^*. However, when the load effect maxima $S_{max,j}$ are iid random variables, which is at least approximately the case if the underlying load process is stationary and has a limited correlation length, the individual $\Pr(F_j^*)$ can be computed as

$$\Pr(F_j^*) \approx \Pr[R(t_j) \leq S_{max}] \tag{4}$$

The only difference to Eq. (3) is that we replaced $S_{max,j}$ with S_{max}, which has the same distribution but is the same random variable for different time intervals.

The cumulative failure probability $\Pr[F(t_j)]$ can be estimated by the probability of the union of the interval failure events up to t_j:

$$\Pr[F(t_j)] = \Pr(F_1^* \cup F_2^* \cup \dots \cup F_j^*) \tag{5}$$

Its bounds are:

$$\max_{k \in [1,\dots,j]} \Pr(F_k^*) \leq \Pr[F(t_j)] \leq 1 - \prod_{k=1}^{j} [1 - \Pr(F_k^*)] \tag{6}$$

It should be noted that the use of the same S_{max} in Eq. (4) is not correct in the context of evaluating Eq. (5). However, Straub et al. (2019) show how the results of Eq. (4) can be utilized to estimate $\Pr[F(t_j)]$, by computing $\Pr(F_j^*)$ and accounting for the dependence among the events F_j^*. Hence, being able to evaluate Eq. (4) with computationally cheaper methods can be essential for an efficient computation of $\Pr[F(t_j)]$.

2.2. Dependence among interval failure events

For the case that the capacity $R(t_j)$ decreases monotonically over time, it holds that $\{R(t_j) \leq S_{max}\} \subseteq \{R(t_{j+1}) \leq S_{max}\}$, i.e. failure domains of earlier time intervals are subsets of those in later intervals. Therefore, for the purpose of computing $\Pr(F_j^*)$ following Eq. (4), we can postulate that the interval failure events are nested $F_j^* \subseteq F_{j+1}^*$, as illustrated in Figure 1. In reality, the events are of course not nested, but that is not relevant when computing only the marginal $\Pr(F_j^*)$. The $\Pr(F_j^*)$ of later time intervals are larger and thus are cheaper to be evaluated by sampling-based approaches. This motivates a backward calculation scheme in which one evaluates $\Pr(F_j^*)$ in reverse time order from the last to the first time interval.

This strategy can be combined with most structural reliability methods, but is particularly well suited for sequential sampling methods. In the following, we describe its implementation coupled with SuS and SIS.

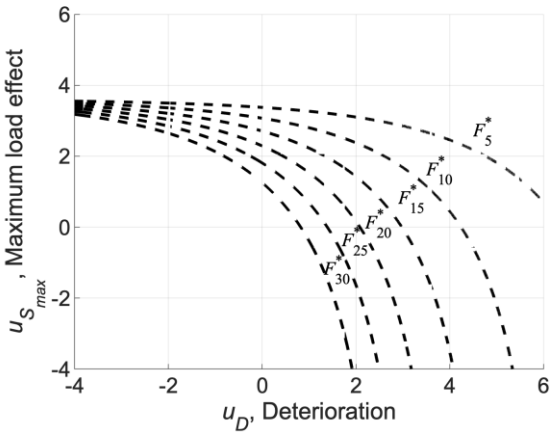

Figure 1: The interval failure events F_j^* in selected time intervals, projected onto the same standard normal outcome space spanned by $u_{S_{max}}$ and u_D. The upper right area of each curve indicates the interval failure domains, which are nested.

2.3. Reverse SuS

When $F_j^* \subseteq F_{j+1}^*$, $\Pr(F_j^*)$ can be expressed by

$$\Pr(F_j^*) = \Pr(F_j^* | F_{j+1}^*) \Pr(F_{j+1}^*) \tag{7}$$

We propose *reverse SuS*, in which Eq. (7) is solved sequentially using Subset Simulation (SuS) in reverse time order. Initially, the interval failure probability in the last time interval is computed using standard SuS. Following Eq. (7), the estimation reduces to $\Pr(F_j^* | F_{j+1}^*)$ in the preceding time intervals. In reverse SuS, the conditional probabilities are readily evaluated via MCS using the samples in F_{j+1}^* if the two adjacent interval failure domains are close, i.e. if the conditional probability is larger than a threshold, e.g. 10%. Otherwise, $\Pr(F_j^* | F_{j+1}^*)$ is estimated by performing a SuS step, in which the samples in F_{j+1}^* are taken as seeds for MCMC.

Figure 2 demonstrates reverse SuS applied to the numerical example in Section 4. In this example, the samples identified for $\Pr(F_{30}^*)$ are readily used up to t_{24} without a need for MCMC. In total, only four subset levels are involved to estimate all $\Pr(F_j^*)$ in all time intervals, $j = 30, 29, \ldots, 1$.

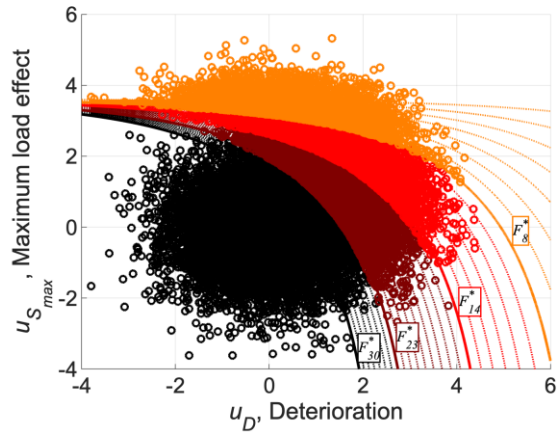

Figure 2: An illustration of reverse SuS where the variation of colors (from dark to light) indicates its progress in reverse time order. The lines depict F_j^*; at the solid ones (conditional) MCMC samples (circles) are obtained while at the dotted ones the already generated samples of the same color are used to estimate $\Pr(F_j^* | F_{j+1}^*)$.

The reverse SuS algorithm is:

Notation:
M: The index of the last time interval
n_s: The number of samples per subset level
p_0: The fraction of accepted samples as seeds per subset level (typically 10%)
$\mathbf{X}_j$: The samples in F_j^*
n_j: The number of samples in $\mathbf{X}_j$

1) Perform standard SuS to compute $\Pr(F_M^*)$
FOR $j = M - 1 : -1 : 1$
  2) Find samples $\mathbf{X}_{j+1}$ among $\mathbf{X}_j$
  IF $n_j \geq n_s \cdot p_0$,
    3) $\Pr(F_j^* | F_{j+1}^*) = \frac{n_j}{n_{j+1}}$
  ELSE
    4) Compute $\Pr(F_j^* | F_{j+1}^*)$ through standard SuS by taking as seeds the $\mathbf{X}_{j+1}$ with the $n_s \cdot p_0$ smallest limit state function values
  ENDIF
  5) Compute the interval failure probability by
$$\Pr(F_j^*) = \Pr(F_j^* | F_{j+1}^*) \Pr(F_{j+1}^*)$$
ENDFOR

The SuS parameters are selected as $n_s = 1000$ and $p_0 = 0.1$. The standard SuS and MCMC methods are here based on (Papaioannou et al. 2015; Straub et al. 2016), but any available algorithm can be implemented.

2.4. Reverse SIS

The backward calculation scheme is combined with Sequential Importance Sampling (SIS) proposed in (Papaioannou et al. 2016).

The proposed reverse SIS computes the interval failure probabilities using Eq. (4) also in reverse time order. Initially, the optimal Importance Sampling (IS) density is evaluated for the last time interval. For earlier time intervals, the algorithm checks if the IS density available from the later time interval is sufficiently close to the current interval failure domain. In that case, the interval failure probabilities are simply computed by evaluating the already generated samples from the IS density. Otherwise, the current IS density is taken as the initial proposal density and a new optimal IS density is sought following the standard SIS procedure.

Figure 3 illustrates the interval failure events and the associated sequential IS densities identified by reverse SIS.

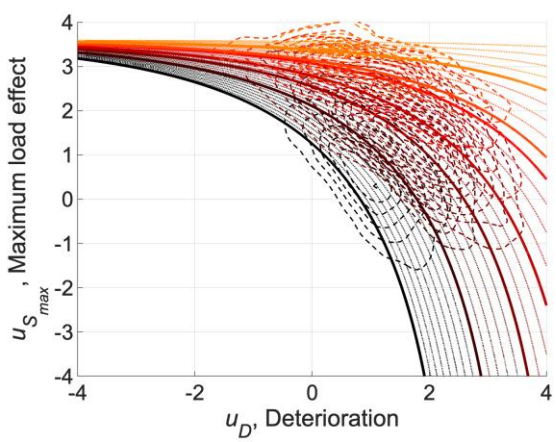

Figure 3: An illustration of reverse SIS where the variation of colors (from dark to light) reflects the sequence in reverse time order. The lines depict F_j^*; at the solid ones, the optimal IS densities (contours) are identified through MCMC while at the dotted ones the already identified IS densities are utilized.

The algorithm is summarized below. It is formulated with the standard normal $\mathbf{U}$, i.e. for the problem transformed from $g(\mathbf{X})$ to $G(\mathbf{U}) = g[T^{-1}(\mathbf{U})]$, wherein T is a suitable transformation from $\mathbf{X}$ to $\mathbf{U}$, and T^{-1} is its inverse.

Notation
M: The index of the last time interval
η_j: The optimal IS density found in t_j
$\mathbf{u}_j$: The samples generated with η_j
$\hat{P}_j$: The normalizing constant of η_j
$G(\cdot)$: The interval failure limit state function in standard normal space

1) Perform standard SIS to compute $\Pr(F_M^*)$

FOR $j = M-1{:}-1{:}1$
4) Check convergence of η_{j+1} to F_j^*
IF convergence,
5) Estimate the interval failure probability by

$$\Pr(F_j^*) = \hat{P}_{j+1} \cdot E\left[I\left[G(\mathbf{u}_{j+1}, t_j) \le 0\right] \cdot \frac{\varphi(\mathbf{u}_{j+1})}{\eta_{j+1}(\mathbf{u}_{j+1}, t_j)}\right]$$

6) Accept samples, parameters and IS density

$$\mathbf{u}_j = \mathbf{u}_{j+1}, \hat{P}_j = \hat{P}_{j+1}, \eta_j = \eta_{j+1}$$

ELSE,
7) Perform standard SIS to identify η_j from η_{j+1}
8) Compute the interval failure probability by

$$\Pr(F_j^*) = \hat{P}_j \cdot E\left[I\left[G(\mathbf{u}_j, t_j) \le 0\right] \cdot \frac{\varphi(\mathbf{u}_j)}{\eta_j(\mathbf{u}_j, t_j)}\right]$$

ENDIF
ENDFOR

3. FAILURE LIMIT STATE FUNCTION REFORMULATED FOR TIME TO FAILURE

In this section, we propose a method that we denote *SuS for* t.

In some instances, it is possible and convenient to reformulate the interval failure event F_j^* in a way that the time to failure can be described explicitly in function of t, such that:

$$F_j^* \approx \{g(\mathbf{X}, t_j) \le 0\} = \{h(\mathbf{X}) \le f_t(t_j)\} \quad (8)$$

wherein h is the reformulated limit state function independent of time, and f_t is a function involving no random variables but only the time parameter t_j. In the simplest case it is $f_t(t_j) = t_j$.

Standard SuS is employed to compute the interval failure probability for the first interval, $\Pr(F_1^*)$, in which the probability is lowest. The probabilities of all other intervals can then be obtained as a side product without any further limit state function calls. To this end, the intermediate thresholds of the SuS computations are compared with $f_t(t)$. At a given subset level k, with associated probability p_k (e.g. 10^{-1}, 10^{-2}, …) and threshold b_k, the corresponding t is found by setting

$$f_t(t) = f_t(t_1) + b_k \tag{9}$$

The resulting t is the time value at which the interval failure probability reaches p_k. The interval failure probabilities at t_j, e.g. yearly values, can be estimated by interpolating the obtained values.

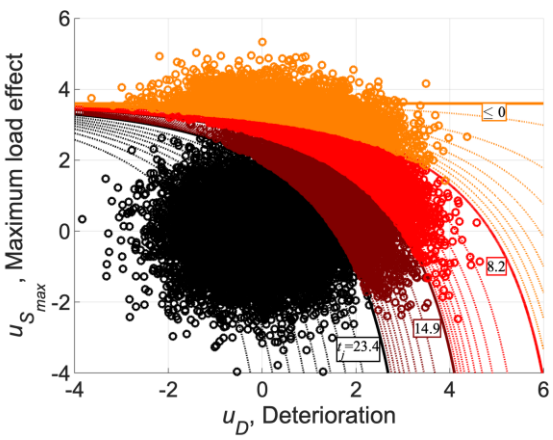

Figure 4: An illustration of the SuS for t method where the variation of colors (from dark to light) indicates the advance of subset levels. The curves depict F_j^* where the solid ones involve new subset levels while the dotted ones are readily identified based on samples from the existing subset levels. The circles are the generated samples, whose colors correspond to the associated F_j^*.

To enhance the accuracy of $\Pr(F_j^*)$ estimates, we identify further intermediate threshold values that correspond to probabilities in between standard subset levels; e.g. at $9 \cdot 10^{-2}$, $8 \cdot 10^{-2}$,…, $2 \cdot 10^{-2}$ probability. This does not require any additional evaluation of limit state functions, hence the additional computational costs are negligible.

Figure 4 illustrates the proposed method by showing the samples and the associated F_j^*, which are identified subsequently through one run of SuS. Figure 5 shows how the obtained probabilities are used to approximate $\Pr(F_j^*)$ in yearly interval.

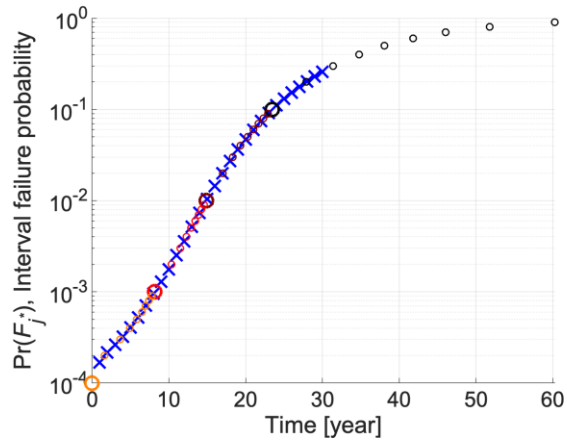

Figure 5: The interval failure probability estimated by the SuS for t method. The circles of the same color are found at each subset level while only the bigger ones involve new subset levels. The blue x-points are the interpolated values on yearly basis.

4. NUMERICAL INVESTIGATION

4.1. Problem definition

We consider a generic structure subject to deterioration and time-varying load effects. Its interval failure event is represented by a time-invariant limit state function g:

$$g(D, S_{max,j}, t_j) = r_0 - k_1 \cdot D \cdot {t_j}^{k_2} - S_{max,j} \tag{10}$$

r_0 is the (unitless and normalized) initial structural capacity assumed to be deterministic. The second term models the degradation of structural capacity over time; k_1 indicates the rate of deterioration, k_2 determines the shape of deterioration curve, and D represents the uncertainty of k_1. Time is discretized in yearly intervals, with $t_j = j,\ j = 1, 2, \ldots, 30$. We set k_1 and k_2 such that the expected remaining capacity in the last time interval becomes 60% of its initial

value. $S_{max,j}$ are the (unitless and normalized) annual maxima of load effects, which are assumed iid. The chosen parameter values are summarized in Table 1.

Table 1: Model parameters.

Parameter	*Type*	*Value*
r_0	Deterministic	100
D	Lognormal	$\mu_D = 1, \sigma_C = 0.4$
$S_{max,j}$	Lognormal	$\mu_S = 50, \sigma_S = 10$
k_1	Deterministic	0.7
k_2	Deterministic	1.2

4.2. Lifetime reliability

The target structure is analyzed with five methods; standard SuS, reverse SuS, standard SIS, reverse SIS, and SuS for t. 1000 samples are generated at each subset level and at each iteration of SIS. The interval failure probabilities $\Pr(F_j^*)$ obtained by these methods are used to estimate the cumulative failure probability $\Pr[F(t_j)]$ following (Straub et al. 2019). That requires estimates of the correlations among interval failure margins, which are available from all investigated methods. For each method, computations are repeated 100 times to obtain estimates of the coefficient of variations of the results.

In Figure 6, we show the mean estimates of $\Pr[F(t_j)]$ evaluated by standard SuS, along with its upper and lower bounds computed by Eq. (6). Note that the upper bound corresponds to the case when uncertainty on the demand $S_{max,j}$ governs the reliability and thus all F_j^* are mutually independent. In contrast, the lower bound, which is identical to $\Pr(F_j^*)$, implies the case when uncertainty on the resistance $R(t_j)$ governs the reliability that all F_j^* are fully dependent. The results of Figure 6 indicate that relying on interval failure probabilities and simple bounds does not allow to evaluate accurate lifetime reliability estimates over the entire lifespan.

The mean estimates of $\Pr[F(t_j)]$ obtained by the five methods are compared in Figure 7. All methods give similar estimates with minor discrepancies that can be explained by sampling uncertainty.

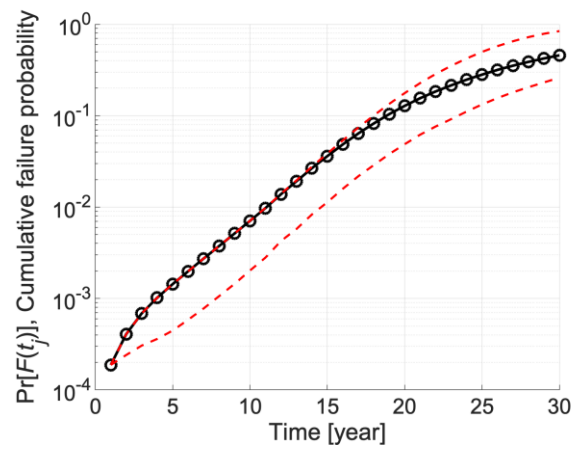

Figure 6: Cumulative failure probability (black solid line with circles) together with the upper and lower bounds (red dashed lines).

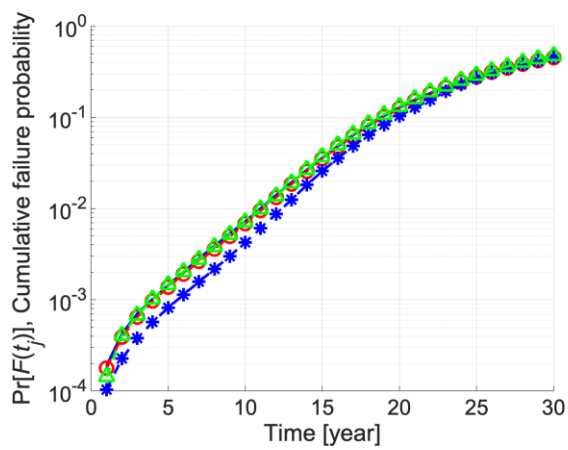

Figure 7: Cumulative failure probability estimated with different methods; red solid line by standard SuS, blue solid line by standard SIS, red dashed line with circles by reverse SuS, blue dashed line with asterisks by reverse SIS, green dashed line with triangles by SuS for t method.

4.3. Computational efficiency

The number of function evaluations (NFE) is used to measure the computational cost of the different methods. In Figure 8, we present the mean NFE spent in each time interval, evaluated as the average of 100 repeated analyses. The results of SuS for t are not shown here because with this method it is not meaning to assign the NFE to yearly time intervals.

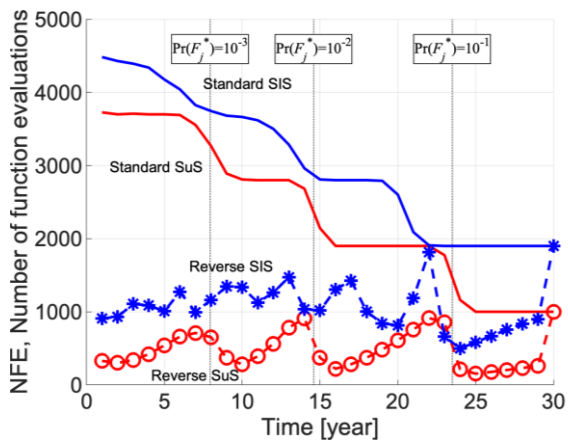

Figure 8: The NFE estimated in each time interval.

Figure 9 shows the mean total NFE required to compute the reliability over the entire lifespan. Implementing the proposed methods reduces the cumulative NFE substantially; by around 80% for reverse SuS and around 65% for reverse SIS. SuS for t method exhibits the best performance, with a cumulative NEF of only about 4%~5% of those required by standard SuS and SIS.

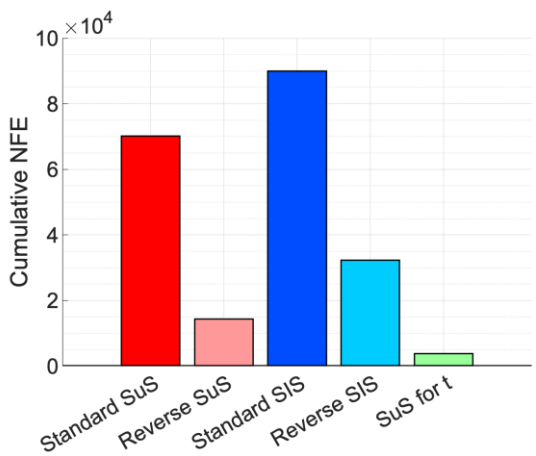

Figure 9: Cumulative NFE by each method.

4.4. Accuracy

We compare the accuracy of the implemented methods. Figure 10 shows 95% credible intervals (CI) of the cumulative failure probabilities evaluated from the 100 repeated runs. In general, the proposed methods lead to slightly larger credible intervals compared to the corresponding standard methods. This implies that the sequential and conditional sampling steps lead to an additional (and undesired) correlation among the samples generated in different time intervals.

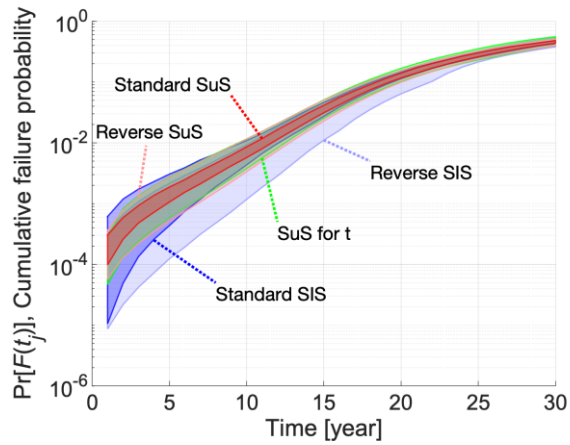

Figure 10: 95% credible interval of $\Pr[F(t_j)]$.

5. SUMMARY AND CONCLUSION

In this contribution, we proposed two computational schemes for efficient computation of the lifetime reliability of deteriorating structures. The first scheme solves sets of time-invariant reliability problems sequentially and in reverse time order, which facilitates to evaluate the nested interval failure domains efficiently. This scheme was implemented through Subset Simulation (SuS) and Sequential Importance Sampling (SIS), but other sequential sampling methods may be considered, e.g. Cross-entropy-based adaptive importance sampling (Wang and Song 2016; Geyer et al. 2019). The second scheme is based on reformulating the failure limit state function such that the time to failure (or a function thereof) can be treated as a threshold, which can be exploited in SuS. In this way, a series of interval failure probabilities are obtained by one standard run of SuS. The numerical investigations showed that the proposed methods are able to obtain accurate estimates of failure probability with substantially reduced computational efforts, with slightly reduced accuracy. The proposed methods can also be applied to reliability updating, particularly when applying Bayesian Updating with Structural reliability methods (BUS) (Straub and Papaioannou 2015). The effectiveness of reverse SuS in solving such Bayesian updating problems

have been demonstrated for the reliability analysis of a ship cross-section subject to spatially variable corrosion in (Kim and Straub 2019).

6. ACKNOLEGEMENTS

The research leading to these results has received funding from the SAFEPEC project under the European Union's FP7 programme.

7. REFERENCES

Andrieu-Renaud, C., Sudret, B., and Lemaire, M. (2004). "The PHI2 method: a way to compute time-variant reliability." *Reliability Engineering & System Safety*, 84(1), 75-86.

Geyer, S., Papaioannou, I., and Straub, D. (2019). "Cross entropy-based importance sampling using Gaussian densities revisited." *Structural Safety*, 76, 15-27.

Kim, H.-J., and Straub, D. (2019). "Reliability analysis of inspected ship structures subject to spatially variable corrosion." *Marine Structures - under review*.

Lentz, A., Defaux, G., and Rackwitz, R. (2004). "Principles of Reliability Calculations for Deteriorating Structures." *Life-Cycle Performance of Deteriorating Structures: Assessment, Design and Management*, 92-101.

Melchers, R. E., and Beck, A. T. (2018). *Structural reliability analysis and prediction*, John Wiley & Sons.

Papaioannou, I., Betz, W., Zwirglmaier, K., and Straub, D. (2015). "MCMC algorithms for subset simulation." *Probabilistic Engineering Mechanics*, 41, 89-103.

Papaioannou, I., Papadimitriou, C., and Straub, D. (2016). "Sequential importance sampling for structural reliability analysis." *Structural safety*, 62, 66-75.

Rackwitz, R. (1998). "Computational techniques in stationary and non-stationary load combination—a review and some extensions." *Journal of Structural Engineering*, 25(1), 1-20.

Schneider, R., Thöns, S., and Straub, D. (2017). "Reliability analysis and updating of deteriorating systems with subset simulation." *Structural Safety*, 64, 20-36.

Straub, D., and Papaioannou, I. (2015). "Bayesian updating with structural reliability methods." *Journal of Engineering Mechanics*, 141(3), 04014134.

Straub, D., Papaioannou, I., and Betz, W. (2016). "Bayesian analysis of rare events." *Journal of Computational Physics*, 314, 538-556.

Straub, D., Schneider, R., Bismut, E., and Kim, H.-J. (2019). "Reliability analysis of deteriorating structures." *Structural Safety - under review*.

Val, D. V., and Melchers, R. E. (1997). "Reliability of deteriorating RC slab bridges." *Journal of structural engineering*, 123(12), 1638-1644.

Wang, Z., and Song, J. (2016). "Cross-entropy-based adaptive importance sampling using von Mises-Fisher mixture for high dimensional reliability analysis." *Structural Safety*, 59, 42-52.